

To appear in *Spitzer* First Results ApJ Supplement

The NGC 7129 Young Stellar Cluster: A Combined *Spitzer*, MMT, and 2MASS Census of Disks, Protostars, and Outflows

Robert A. Gutermuth¹, S. Thomas Megeath², James Muzerolle³, Lori E. Allen², Judith L. Pipher¹, Philip C. Myers², & Giovanni G. Fazio²

ABSTRACT

We present the analysis of seven band (1.2 to 8 μm) ground and space-based imaging of the NGC 7129 young stellar cluster from FLAMINGOS on MMT, 2MASS, and the Infrared Array Camera (IRAC) on the *Spitzer Space Telescope*. An analysis of the $H - [4.5]$ vs. $J - H$ colors reveals 84 objects with circumstellar disks. Of these, 42 are located within the cluster core, a 0.5 pc (100'') radius region of enhanced stellar surface density. From a luminosity and extinction limited sample of the stars within the cluster core boundary we have determined that $54\% \pm 14\%$ have circumstellar disks. Finally, we report the detection of several resolved outflows in the IRAC 4.5 μm mosaic.

Subject headings: pre-main sequence — stars: formation — infrared:stars

1. Introduction

Excess emission at infrared wavelengths has been frequently used to identify those stars that have circumstellar disks. Lada et al. (2000) have shown that disk surveys that utilize 1-2.5 μm photometry exclusively are usually incomplete, and only by inclusion of longer wavelength photometry can a more complete disk sample be achieved. Such samples, once obtained, allow unbiased measurements of the fraction of sources with circumstellar disks in a young stellar cluster. Combined with spectroscopically-derived stellar ages, cluster

¹Department of Physics and Astronomy, University of Rochester, Rochester, NY 14627
(rguter@astro.pas.rochester.edu)

²Harvard-Smithsonian Center for Astrophysics, Mail Stop 42, 60 Garden Street, Cambridge, MA 02138

³Steward Observatory, University of Arizona, 933 N. Cherry Ave. Tucson, AZ 85721

disk fractions may provide insight into the average disk lifetime (Haisch, Lada, & Lada 2001b). Surveying multiple and more distant clusters with ground-based *L*-band imaging is impractical however, as atmospheric emission severely limits sensitivity.

Using the Infrared Array Camera (IRAC) onboard the *Spitzer Space Telescope* (Werner et al. 2004), we can efficiently observe at 3-8 μm with dramatically improved sensitivity, enabling us to obtain a significant census of the YSO population in young stellar clusters. Specifically, the 4.5 μm channel on IRAC has optimal sensitivity to both photospheric and disk emission. When combined with ground-based *JHK* imaging, these new data allow unbiased measurements of the disk fractions of young stellar clusters at distances as large as 1 kpc, increasing the number of clusters that can be studied this way significantly. In this paper, we present just such a young stellar object (YSO) census for the star forming region NGC 7129 to demonstrate the capabilities of IRAC/*Spitzer*.

Located at a distance of 1 kpc¹ (Racine 1968), NGC 7129 is a region of bright reflection nebulosity at optical wavelengths, illuminated by the Be stars BD+65°1637 and BD+65°1638. These two intermediate mass stars are part of a cluster of low mass stars (Hodapp 1994) which occupies a cavity west of a kidney-shaped molecular cloud (Ridge et al. 2003). The cavity is sharply defined in both CO and submillimeter emission (Font, Mitchell, & Sandell 2001), and the cavity wall is seen as a nebulous filament detected at both optical and near IR wavelengths. A third massive member, LkH α 234, lies to the east of the main cluster on the edge of the cavity. An optical jet pointing southwest into the cavity has been associated with it (Ray et al. 1990) or one of its companions (Weintraub et al. 1996) and may be the counter-jet to a red-shifted molecular outflow lobe detected to the northeast. Three arcminutes to the south of the cluster lies FIRS2, a deeply embedded intermediate-mass protostellar object located at the primary peak in ^{13}CO emission (Bechis et al. 1978) and associated with a multipolar molecular outflow (Fuente et al. 2001). There are several known Herbig-Haro objects in and around the region, many of which are associated with sites of outflow activity (Edwards & Snell 1983; Hartigan & Lada 1985).

¹The adopted distance of 1 kpc is derived from from high resolution spectroscopy and optical photometry of one cluster member (Racine 1968); other estimates in the literature, ranging from 0.9 kpc by Ábrahám, Balázs, & Kun (2000) to 1.25 kpc by Shevchenko & Yakubov (1989), bracket the 1 kpc value. The adopted distance does not affect our analysis.

2. Observations

For information on the IRAC instrument, see Fazio et al. (2004). The IRAC/*Spitzer* observations were taken as part of the Spitzer young stellar cluster survey. The observations are described in detail by Megeath et al. (2004).

Near IR observations of the region in the J (1.2 μm), H (1.6 μm), and K_s (2.2 μm) wavebands were obtained by the authors on June 15, 2001 using the FLAMINGOS instrument (Elston 1998) on the 6.5 meter MMT Telescope. A 2×2 position raster was used to make a $9' \times 9'$ mosaic. Five dithered mosaics were obtained in each band, for a total exposure time of 75 seconds at J , H , and K_s . The data were processed using custom IDL routines developed by the authors for ground-based near IR data reduction which include modules for linearization, flat-field creation and application, background frame creation and subtraction, distortion measurement and correction, and mosaicking.

Point source detection and aperture photometry of all point sources were carried out using PhotVis version 1.09, an IDL GUI-based photometry visualization tool developed by Gutermuth. PhotVis utilizes DAOPHOT modules ported to IDL as part of the IDL Astronomy User's Library (Landsman 1993). Detections were visually inspected and those that were identified as structured nebulosity were considered non-stellar and rejected. Radii of the apertures and inner and outer limits of the sky annuli were 1'', 2'', and 3.2'' respectively for the near IR data and 2.4'', 2.4'', and 7.2'' respectively for the IRAC data. FLAMINGOS photometry was calibrated by minimizing residuals to corresponding 2MASS detections, using only those objects with $H - K_s < 0.6$ mag to minimize color differences in the 2MASS and FLAMINGOS filter sets. Photometry for stars that were non-linear or saturated in the FLAMINGOS data were replaced with the appropriate 2MASS measurements in the final analysis. IRAC photometry was calibrated using large aperture measurements of several standard stars from observations obtained in flight. An additional correction was derived and applied for each channel to correct for the smaller apertures used in this study.

3. Results

The four-color composite IRAC image is shown in Figure 1. We note two different types of extended emission. The brightest and most extended nebulosity is the reflection nebula, which is most prominent in the 8.0 μm (red) band. This band includes the 7.7 μm emission feature commonly attributed to PAHs. In addition, 4.5 μm -bright (green) structured shocks and knots associated with outflow activity are easily discernible at two sites located south and east of the cavity. The preponderance of outflow activity outside the cluster core suggests

that current star formation activity is ongoing in the molecular cloud.

Centered in the reflection nebulosity is the cluster of stars most apparent in the near IR (Hodapp 1994). Using our K_s –band star counts, we determined the location of the peak local stellar surface density, and measured the radial stellar surface density profile centered on this point. We measured the half-width at half maximum density from this profile to be approximately 0.17 pc, and defined the boundary of the cluster core as a circle centered on the stellar density peak with a radius of three times this distance, or 0.5 pc (Gutermuth et al. 2004).

3.1. Census of Objects with Disks

To identify the population of young, forming stars with IR excess (circumstellar disks) we use an $H - [4.5]$ vs. $J - H$ color-color diagram for all stars detected at J , H , and K_s with photometric uncertainties of less than 0.1 magnitudes and 4.5 μm (Fig. 2b) with photometric uncertainties of less than 0.25 magnitudes². We interpret those that exhibit colors inconsistent with reddened dwarf or giant stars as stars with circumstellar disks. We used the reddening law of Rieke & Lebofsky (1985) for this analysis, interpolated to take into account the filter response of the 4.5 μm channel of IRAC. We have restricted this study to only those objects with dereddened J –band magnitudes less than 16.5, equivalent to the luminosity of a 1 Myr old 0.06 M_\odot or a 3 Myr old 0.08 M_\odot star (Baraffe et al. 1998) at the adopted distance. An age of 3 Myr was chosen as a conservative upper limit for the age of the cluster core population, although it is clear from the presence of protostellar objects reported in this paper and the companion studies that there are much younger stars present in the molecular cloud.

The positions of those objects with IR excess are plotted as green diamonds in Figure 1. We find 84 objects with disks out of a total of 405 objects that are detected in all four bands within the above constraints. Of these, 42 out of the 87 that are located within the cluster core boundary have disks. Note that the cluster core has a significantly higher density of objects with disks compared with the rest of the field even though the 4.5 μm sensitivity is significantly reduced because of the bright nebulosity in the cavity. Nevertheless, the total number of stars with disks detected both inside and outside the cluster core boundary is similar. Most of this peripheral star formation appears to be located in parts of the molecular cloud north, east, and south of LkH α 234. There are also several stars with IR excess near

²Photometric uncertainties take into account varying background toward each star. This component can dominate the 4.5 μm band error estimates.

the western edge of the reflection nebula. These may be young stars with disks from the core that have emerged from the molecular cloud, or they could be background galaxies, planetary nebulae, or AGB stars. The IRAC colors and the number of these potential contaminating objects are currently not well characterized, but given the small number of IR excess sources detected away from the molecular cloud, these contaminants are not expected to alter the deduced disk frequency significantly.

For comparison, red points are also plotted in Figure 1 to mark those YSOs detected and classified using only the four IRAC bands (Megeath et al. 2004; Allen et al. 2004), and white points mark those YSOs detected and classified using the IRAC and MIPS combined colors (Muzerolle et al. 2004). These methods complement each other well, as the longer wavelengths suffer from loss of sensitivity in the bright central nebulosity, whereas the near IR data in this study cannot detect sources in the heavily extinguished regions of the molecular cloud. It is clear in all these studies that in addition to the dense cluster core there is an extended population of young stars predominantly located in the eastern molecular cloud.

3.2. Measuring the Disk Fraction

To achieve an unbiased sample of stars in the NGC 7129 cluster for measurement of the fraction of stars with disks, we first restrict our sample to objects detected at J , H , and K_s wavelengths within the cluster core boundary. We then plot our sample on a $J - H$ vs. J color-magnitude diagram (see Fig. 3), marking the stars which are also detected at $4.5 \mu\text{m}$. Since stars with disks are substantially more luminous at $4.5 \mu\text{m}$, the disk fraction can be overestimated if we select sources on the basis of the IRAC photometry. By basing our sample selection on the dereddened J -band magnitude, which is dominated by the emission from the stellar photosphere (Kenyon & Hartmann 1990), we avoid this bias. Furthermore, by adopting a modest maximum extinction, we are sampling all stars above the magnitude limit within the spatial volume defined by our cluster core boundary and the extinction limit. We choose a dereddened J magnitude upper limit of 15.5, corresponding to the luminosity of a 1 Myr old $0.1 M_\odot$ star or a 3 Myr old $0.2 M_\odot$ star (Baraffe et al. 1998) at the adopted distance, and an extinction upper limit of $A_V = 6$ mag ($A_J = 1.7$ mag). These limits are chosen such that 90% of the stars in the sample have corresponding $4.5 \mu\text{m}$ detections, with the non-detections evenly distributed on the color-magnitude diagram. We also take the same sample from nearby control fields on the edge of our mosaic. From this we estimate 20% of the stars in the final cluster core sample are field stars.

Those stars that remain in our final sample are plotted on the $H - [4.5]$ vs. $J - H$ color-color diagram in Figure 4. All stars to the right and below the reddening vector originating

at the M5 dwarf colors are considered to have excess emission at $4.5 \mu\text{m}$ and therefore circumstellar disks. Of the 62 stars in the final sample, 32 have disks. If 20% of the sample of 62 stars are in fact background stars, then only 50 are probable cluster members, yielding a high estimated disk fraction of 64%. If we reject all those objects within 1 sigma of the M5 reddening vector as before, the total number of objects with disks drops to 27, for a total of $54\% \pm 14\%$. The statistical uncertainty is derived assuming Poisson counting statistics for the number of stars with excesses, the total number of stars in the cluster core, and the number of stars in our control fields used for determining background contamination.

4. Discussion

As demonstrated clearly in Figure 2, combining the longer wavelength IRAC data with the near IR data is a more robust method for the detection of circumstellar disks than JHK -based methods allow. The photospheres of both ordinary stars and young stars are characterized well by J and H bands, but detecting the warm inner disks at K -band is uncertain because of the relative weakness of disk emission compared to that from photospheres at $2.2 \mu\text{m}$. The spectral energy distributions of protostellar disks dominate photospheric SEDs at wavelengths longer than $2.2 \mu\text{m}$, allowing easier detection if adequate sensitivity can be achieved, as has been done with IRAC/*Spitzer*. For disk fraction studies specifically, the $4.5 \mu\text{m}$ channel of IRAC has the ideal combination of sensitivity to both photospheric and disk emission needed for unbiased sampling of the entire stellar population, both with and without disks.

We measure a disk fraction of 54% for the cluster core of NGC 7129. When compared to other long wavelength ($JHKL$) measurements, we note that the disk fraction in NGC 7129 is significantly lower than 80% reported for the Trapezium cluster by Lada et al. (2000) and 86% in NGC 2024 as reported by Haisch, Lada, & Lada (2000). Both of these clusters are considered to be very young ($< 1 \text{ Myr}$). However, our result is fairly close to that found for the 2.3 Myr cluster IC 348, which has a disk fraction of 65% (Haisch, Lada, & Lada 2001a), and the 3.2 Myr cluster NGC 2264 which has 52% (Haisch, Lada, & Lada 2001b). Future work will be focused on measuring the age of the NGC 7129 cluster core to compare with the disk lifetime study presented in Haisch, Lada, & Lada (2001b).

While this study concentrated on the cluster core, the significant number of young stars and protostellar objects outside the core is evidence of active extended star formation in this region. Star counts using our K_s -band photometry in the cluster core and in our control fields suggest there are approximately 80 cluster members down to $K_s = 16$ mag. This sensitivity allows us to reach unattenuated 1-3 Myr old objects down to $0.055 M_\odot$ (Baraffe

et al. 1998). In the periphery of the cluster we estimate the number of stars with disks at 62, through a combination of those reported here and the YSOs reported in the companion papers (Megeath et al. 2004; Muzerolle et al. 2004). Most of those YSOs that are missed in this study are either outside the coverage of the near IR data or are highly embedded and thus missing J –band detections. Clearly, the extended cluster population contains a roughly equal number of stars as the high density cluster core, and thus comprises a significant portion of the total stellar content in NGC 7129.

The bright nebulosity extending from the northeast boundary of the reflection nebula is coincident with a complex of Herbig-Haro objects, several molecular hydrogen knots, and a CO outflow; these data indicate that the nebulosity is probably heated by shocks, and not by radiation from nearby stars. Although the nebulosity is evident in all four IRAC bands, it shows a distinctly different color and structure than the reflection nebula, and is particularly prominent in the $4.5 \mu\text{m}$ band. Since this band contains the CO fundamental and several H_2 lines, the emission in the $4.5 \mu\text{m}$ band probably has a large component from shock heated molecular gas. It is still not known whether this region contains one or multiple outflows, nor is it known which sources are driving the outflow. IRAC and MIPS imaging of NGC 7129 have shown four protostellar (Class I) and two pre-main sequence stars with disks (Class II) within the nebulosity (Megeath et al. 2004; Muzerolle et al. 2004, this work). Given the complex shape of the emission, and the presence of multiple protostellar objects, we find it likely that this nebulosity contains the combined emission from several outflows.

Several distinct outflow arcs traced by $4.5 \mu\text{m}$ -bright knots appear to be associated with FIRS2. The object itself is elongated perpendicular to the extended outflow arcs, suggesting another outflow axis which is resolved as distinct emission knots in our K_s –band image. The observed multipolar nature of this outflow system, in general agreement with the the outflow analysis of Fuente et al. (2001), lends support to the claim by Miskolczi et al. (2001) that FIRS2 is a multiple protostellar system. We note at least one other obvious outflow arc that does not seem to be associated directly with FIRS2. Future work will involve numerical modeling of these resolved outflows to investigate their influence on the star forming environment of the natal molecular cloud.

This work is based on observations made with the *Spitzer Space Telescope*, which is operated by the Jet Propulsion Laboratory, California Institute of Technology under NASA contract 1407. Support for this work was provided by NASA through Contract Number 1256790 issued by JPL/Caltech. Support for the IRAC instrument was provided by NASA through Contract Number 960541 issued by JPL. Ground-based observations reported here were obtained at the MMT Observatory, a joint facility of the Smithsonian Institution and the University of Arizona. FLAMINGOS was designed and constructed by the IR instru-

mentation group (PI: R. Elston) at the University of Florida, Department of Astronomy with support from NSF grant (AST97-31180) and Kitt Peak National Observatory. This publication makes use of data products from the Two Micron All Sky Survey, which is a joint project of the University of Massachusetts and the Infrared Processing and Analysis Center/California Institute of Technology, funded by the National Aeronautics and Space Administration and the National Science Foundation. This research has made use of the SIMBAD database, operated at CDS, Strasbourg, France. Link to the data set used in this analysis: ads/sa.spitzer#0003655168

REFERENCES

Ábrahám, P., Balázs, L. G., & Kun, M., 2000, *A&A*, 354, 645

Allen, L. E., et al., 2004, *ApJS*, this volume

Baraffe, I., Chambrier, G., Allard, F., & Hauschildt, P. H., 1998, *A&A*, 337, 403

Bessell, M. S. & Brett, J. M., 1988, *PASP*, 100, 1134

Bechis, K. P., Harvey, P. M., Campbell, M. F., & Hoffmann, W. F., 1978, *ApJ*, 226, 439

Edwards, S., & Snell, R. L., 1983, *ApJ*, 270, 605

Elston, R., 1998, *Proc. SPIE*, 3354, 404, *Infrared Astronomical Instrumentation*, Albert M. Fowler, ed.

Fazio, G. G. et al. 2004, *ApJS*, this volume

Font, A. S., Mitchell, G. F., Sandell, G., 2001, *ApJ*, 555, 950

Fuente, A., Neri, R., Martin-Pintado, J., Bachiller, R., Rodriguez-Franco, A., & Palla, F., 2001, *A&A*, 366, 873

Gutermuth, R. A., Megeath, S. T., Pipher, J. L., Williams, J. P., Allen, L. E., Myers, P. C., 2004, in preparation

Haisch, K. E., Jr., Lada, E. A., & Lada, C. J., 2000, *AJ*, 120, 1396

Haisch, K. E., Jr., Lada, E. A., & Lada, C. J., 2001, *AJ*, 121, 2065

Haisch, K. E., Jr., Lada, E. A., & Lada, C. J., 2001, *ApJ*, 553, L153

Hartigan, P., & Lada, C. J., 1985, *ApJS*, 59, 383

Hodapp, K. W. 1994, *ApJS*, 94, 615

Kenyon, S. J., & Hartmann, L. W., 1990, *ApJ*, 349, 197

Lada, C. J., Muench, A. A., Haisch, K. E., Jr., Lada, E. A., Alves, J. F., Tollestrup, E. V., & Willner, S. P., 2000, *AJ*, 120, 3162

Landsman, W. B, 1993, Astronomical Data Analysis Software and Systems II, A.S.P. Conference Series, Vol. 52, ed. R. J. Hanisch, R. J. V. Brissenden, and Jeannette Barnes, p. 246

Megeath, S. T., Gutermuth, R. A., Allen, L. E., Pipher, J. L., Myers, P. C., & Fazio, G. G., 2004, *ApJS*, this volume

Miskolczi, B., Tothill, N. F. H., Mitchell, G. F., Matthews, H. E., 2001, *ApJ*, 560, 841

Muzerolle, J., et al., 2004, *ApJS*, this volume

Racine, R., 1968, *AJ*, 73, 233

Ray, T. P., Poetzel, R., Solf, J., & Mundt, R., 1990, *ApJ*, 357, L45

Ridge, N. A.. Wilson, T. L., Megeath, S. T., Allen, L. E., Myers, P. C., 2003, *AJ*, 126, 286.

Rieke, G. H., & Lebofsky, M. J., 1985, *ApJ*, 288, 618

Shevchenko, V. S., & Yakubov, S. D., 1989, *Soviet Astron.*, 33, 370

Weintraub, D. A., Kastner, J. H., Gatley, I., & Merrill, K. M., 1996, *ApJ*, 468, L45

Werner, M. W., et al., 2004, *ApJS*, this volume

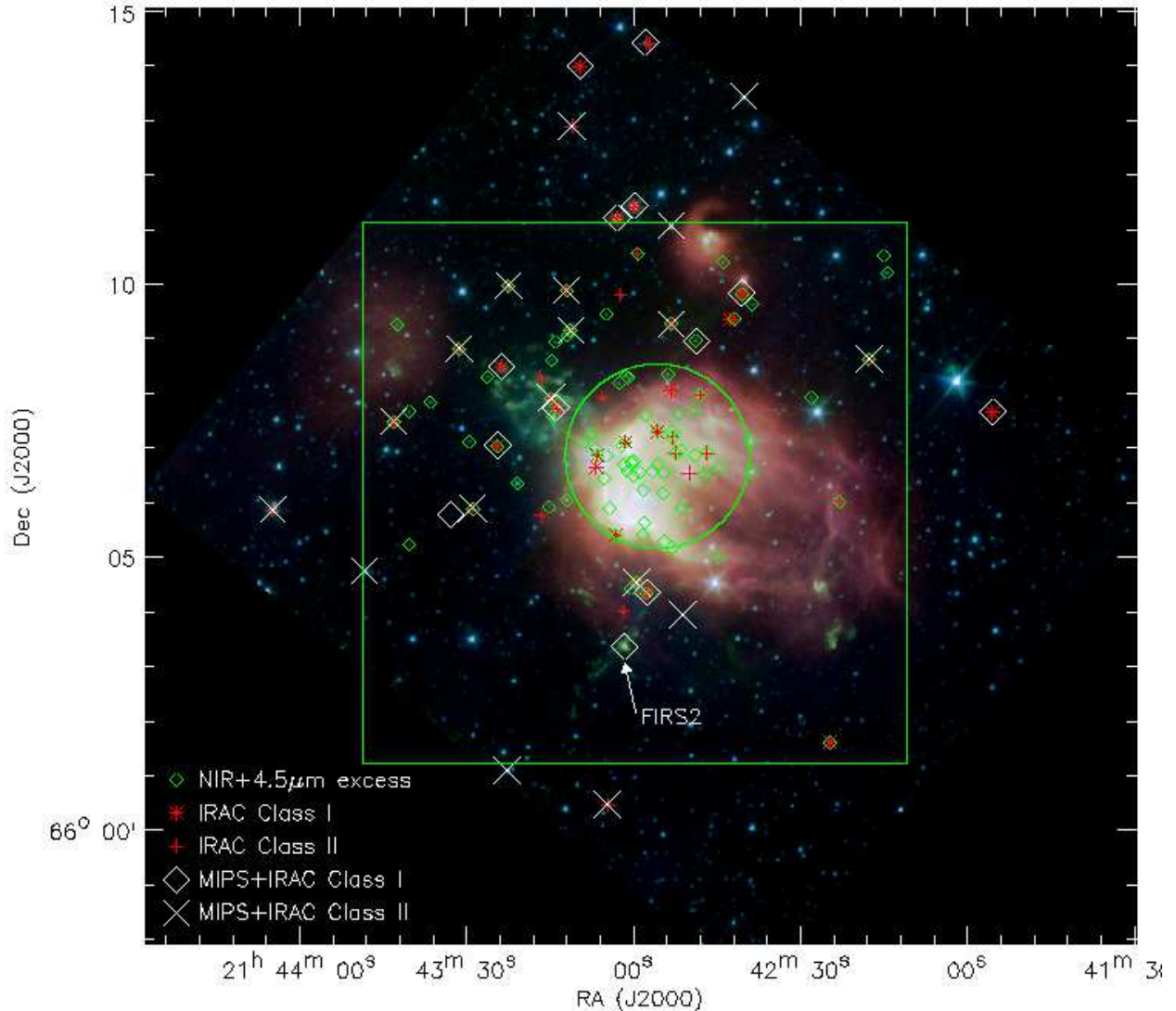


Fig. 1.— IRAC four-color image of NGC 7129. The large green square shows the field of view of the near IR data. The green circle denotes the cluster core boundary as defined in Section 3. The green diamonds are those objects with disks from the $H - [4.5]$ vs. $J - H$ color-color diagram in Fig. 2. Embedded protostars (Class I YSOs) and classical T-Tauri stars (Class II YSOs) reported in the companion papers are also marked. Red asterisks are Class I YSOs and red pluses are Class II YSOs as determined in Megeath et al. (2004) using IRAC photometry alone and YSO modeling from Allen et al. (2004). Large white diamonds are Class I YSOs and large white X's are Class II YSOs from IRAC and MIPS combined photometry in Muzerolle et al. (2004).

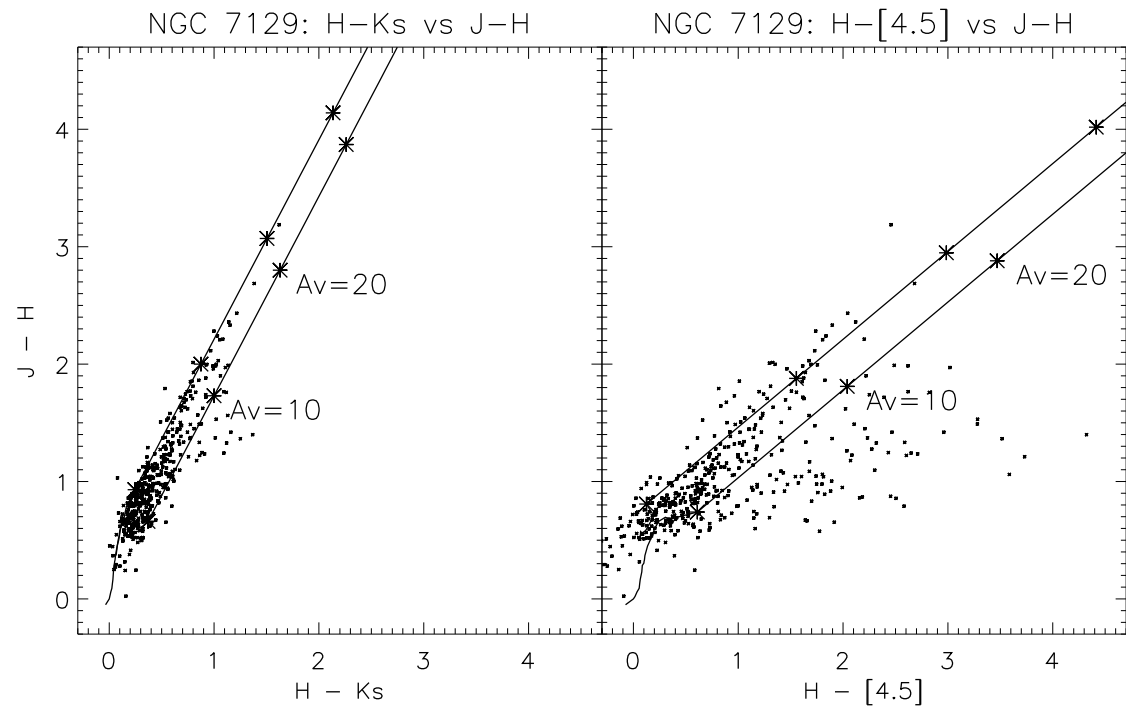


Fig. 2.— JHK_s and $JH[4.5]$ color-color diagrams for the NGC 7129 region. The upper and lower reddening vectors show the Rieke & Lebofsky (1985) reddening law for an M5 giant (Bessell & Brett 1988) and an M5 dwarf respectively, as measured by IRAC and 2MASS (Brian Patten, personal communication). Those objects greater than 1 sigma below and to the right of the lower reddening vector have circumstellar disks.

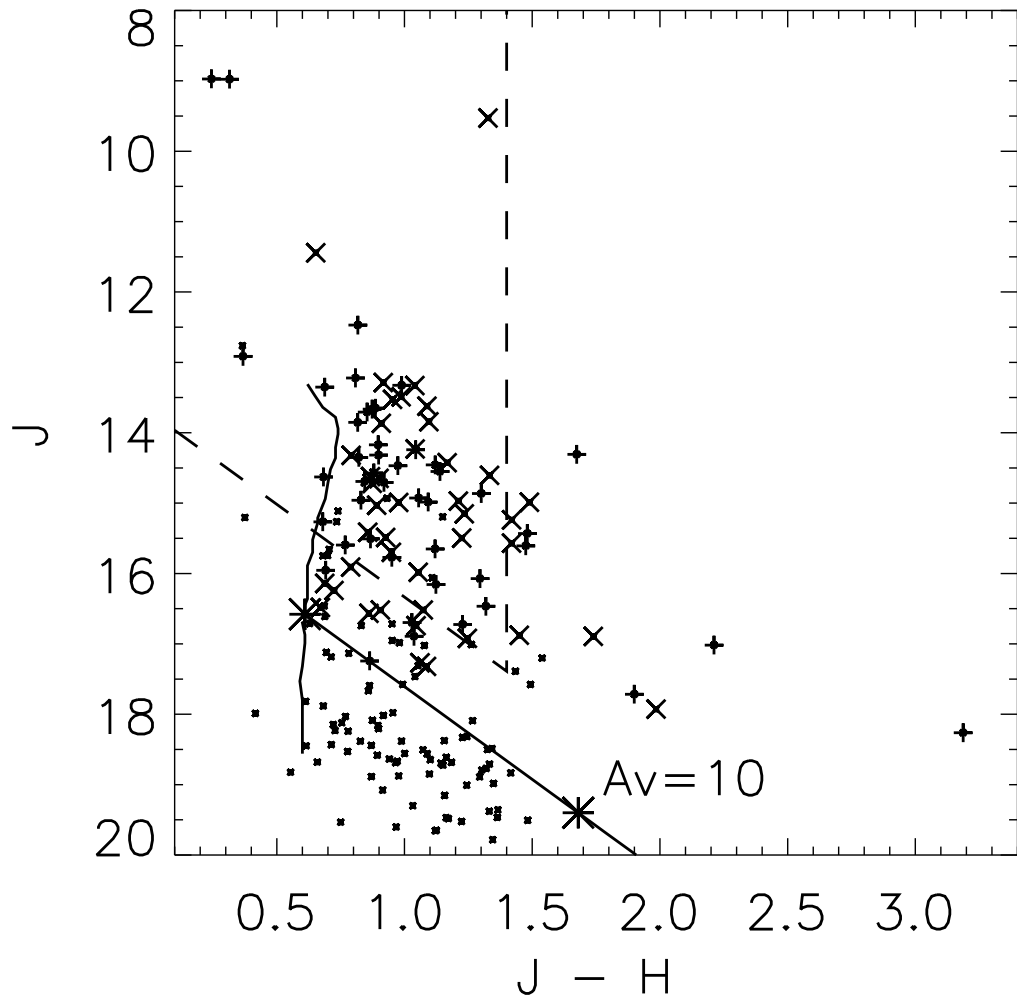


Fig. 3.— $J - H$ vs. J color-magnitude diagram of the objects in the cluster core boundary. Dots are objects only detected at J , H , and K_s but not $4.5 \mu\text{m}$. Crosses and pluses mark those objects that have been detected at JHK and $4.5 \mu\text{m}$ and have $4.5 \mu\text{m}$ excess emission and no excess emission respectively. For comparison, the near vertical curve is the 3 Myr isochrone of Baraffe et al. (1998) for stars between $1 M_{\odot}$ and $0.025 M_{\odot}$. The slanted line is the Rieke & Lebofsky (1985) reddening vector for a $0.08 M_{\odot}$ star. The slanted dashed line denotes the limiting dereddened J magnitude corresponding to $0.2 M_{\odot}$ and the vertical dashed line denotes the limiting extinction of $A_V = 6$ mag, chosen to give an unbiased sample for measuring the disk fraction.

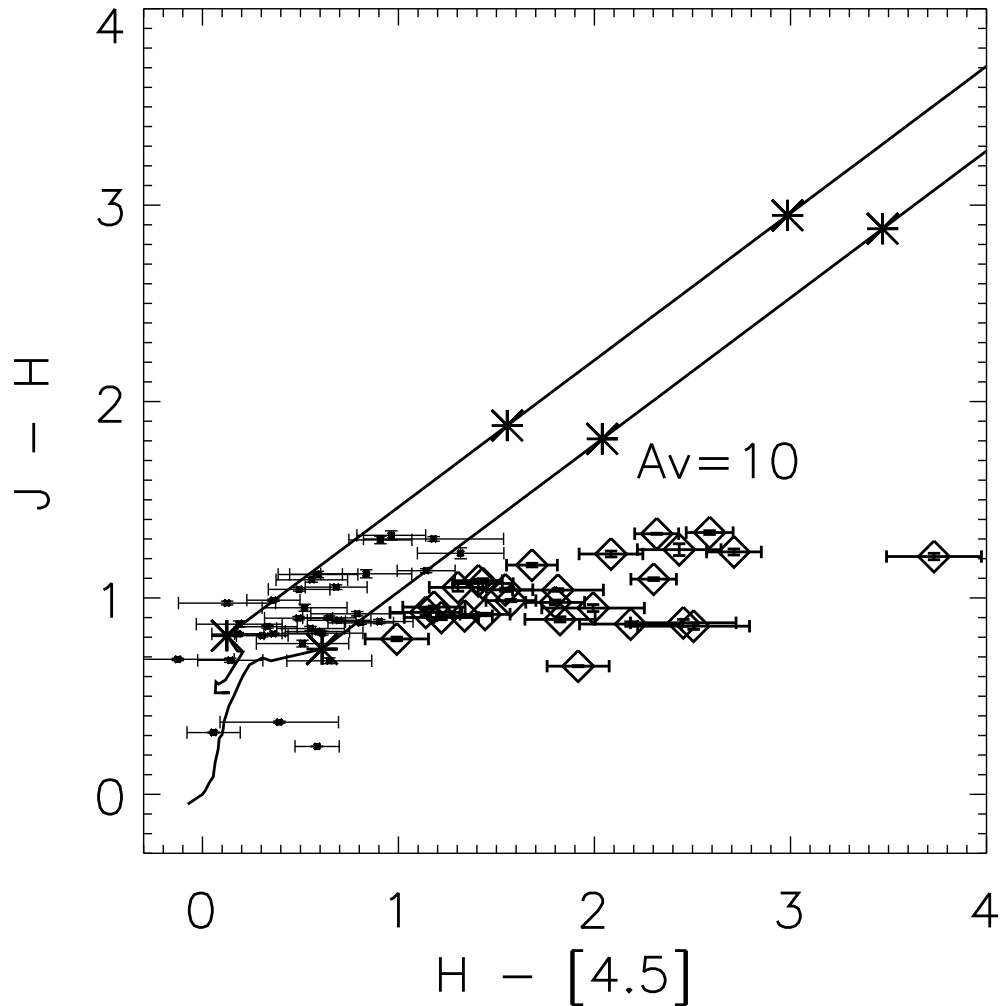


Fig. 4.— $H - [4.5]$ vs. $J - H$ diagram of the final luminosity and extinction limited sample with photometric uncertainties overlaid. The error bars take into account varying sky background toward each star. This component can dominate the uncertainties in the $4.5 \mu\text{m}$ band. Reference colors and reddening vectors are the same as those described for Fig. 2b. Those objects plotted with diamonds have disks. From this plot we measure a disk fraction of $54\% \pm 14\%$.